Article

pubs.acs.org/Biomac

High Molecular Weight Poly(butylene succinate-*co*-butylene furandicarboxylate) Copolyesters: From Catalyzed Polycondensation Reaction to Thermomechanical Properties

Linbo Wu,[†,‡] Rosica Mincheva,[‡] Yutao Xu,[†] Jean-Marie Raquez,[‡] and Philippe Dubois*[,‡]

[†]State Key Laboratory of Chemical Engineering at ZJU, Department of Chemical and Biological Engineering, Zhejiang University, Hangzhou 310027, China

[‡]Laboratory of Polymeric and Composite Materials (LPCM), Center of Innovation and Research in Materials and Polymers (CIRMAP), University of Mons, Mons 7000, Belgium

ABSTRACT: Novel potentially biobased aliphatic−aromatic copolyesters poly(butylene succinate-*co*-butylene furandicarboxylate) (PBSFs) in full composition range were successfully synthesized from 2,5-furandicarboxylic acid (FA), succinic acid (SA), and 1,4-butanediol (BDO) via an esterification and polycondensation process using tetrabutyl titanate (TBT) or TBT/La(acac)$_3$ as catalyst. The copolyesters were characterized by size exclusion chromatography (SEC), Fourier transform infrared (FTIR), ^{1}H NMR, differential scanning calorimetry (DSC) and thermogravimetric analysis (TGA), and their tensile properties were also evaluated. The weight average molecular weight (M_w) ranges from 39 000 to 89 000 g/mol. The copolyesters are random copolymers whose composition is well controlled by the feed ratio of the diacid monomers. PBSFs have excellent thermal stability. The glass transition temperature (T_g) increases continuously with ϕ_{BF} and agrees well with the Fox equation. The crystallizability and T_m decrease with increasing butylene furandicarboxylate (BF) unit content (ϕ_{BF}) from 0 to 40 mol %, but rise again at ϕ_{BF} of 50−100 mol %. Consequently, the tensile modulus and strength decrease, and the elongation at break increases with ϕ_{BF} in the range of 0−40 mol %. At higher ϕ_{BF}, the modulus and strength increase and the ultimate elongation decreases. Thus, depending on ϕ_{BF}, the structure and properties of PBSFs can be tuned ranging from crystalline polymers possessing good tensile modulus (360−1800 MPa) and strength (20−35 MPa) to nearly amorphous polymer of low T_g and high elongation (~600%), and therefore they may find applications in thermoplastics as well as elastomers or impact modifiers.

INTRODUCTION

Because of increasing worldwide concern about the shortage of nonrenewable petroleum resources, biobased monomers and polymers made from annually renewable resources have attracted much attention from both academic and industrial fields in the past decades.[1−6] Some biobased polymers such as poly(L-lactic acid) are also biodegradable.[7,8] As the production, application, and resource regeneration of such biobased biodegradable polymer can make up a sustainable industrial ecological cycle and reduce net carbon emission, research and development (R&D) of a new biobased biodegradable polymer has become very attractive and desirable.

In recent years, a burgeoning surge in conversion and utilization of biomass and rapid development in the biorefinery industry offer a vast number of opportunities in the synthesis of new biobased monomers and polymers.[2−6] 2,5-Furandicarboxylic acid (FA) is such a biobased aromatic diacid monomer. It has been screened to be one of the most important building blocks or top value-added chemicals derived from biomass by the U.S. Department of Energy.[9] FA can be produced from cellulose or semicellulose through a multistep process including bioconversion, dehydration, and oxidation in which hexose and 5-hydroxymethylfurfural are important intermediates.[10−13] Its physical and chemical properties are close to those of terephthalic acid (TPA), and its price in the future is estimated to be comparable to that of TPA.[14] Therefore, FA is a promising monomer for new polyesters and other polymers.[14−21] Due to recent successful breakthroughs in the R&D of FA,[10−13] several polyesters of FA and various diols have been reported.[14,17−21] Among them, poly(ethylene furandicarboxylate) (PEF) is deemed as a good counterpart of poly(ethylene terephthalate) (PET), especially for bottle application.[17] Copolymerizing FA with aliphatic diacids such as succinic (SA) or adipic (AA) acid and diols such as 1,4-butanediol (BDO) will result in new aliphatic−aromatic copolyesters. Such copolyesters will be potentially biobased, as SA, AA, and BDO can also be produced from biomass although they are mainly produced from petroleum resources at present. Moreover, their properties including biodegradability might be comparable to the well-known copolyesters poly(butylene succinate-*co*-butylene terephthalate) (PBST) and poly(butylene adipate-co-butylene terephthalate) (PBAT)[22−24] within an appropriate composition range. However, except that Oishi et al. reported chemical modification of PBS recently by introducing less than 5 mol % butylene furandicarboxylate (BF) unit using dibutyl furandicarboxylate,[25] there is no report on the synthesis and properties of FA-based copolyesters.

In this work, we synthesized poly(butylene succinate-co-butylene furandicarboxylate)s (PBSFs) copolyesters in full composition range via direct esterification and polycondensation routes. The copolyesters were characterized by size exclusion chromatography (SEC), Fourier transform infrared

Received: July 6, 2012
Revised: July 20, 2012
Published: July 25, 2012

(FTIR), ^{1}H NMR, differential scanning calorimetry (DSC), thermogravimetric analysis (TGA), and their tensile properties were also assessed. It was found that PBSF possesses excellent thermal and mechanical properties, and its behavior ranges from crystalline thermoplastics to amorphous elastomer-like polymers depending on composition.

EXPERIMENTAL SECTION

Materials. SA (99%, Kosher), BDO (99%, Kosher), tetrabutyl titanate (TBT, Across) and lanthanum(III) acetylacetonate hydrate ($La(acac)_3{\cdot}H_2O$, Sigma) were all used as received. FA (99.5% according to the provider) was purchased from Satar Chem., China. It was further purified by refluxing a mixture of FA, 4-fold acetic acid, and 1-fold water for 4 h, filtration, washing with water, and drying under vacuum to constant weight.

Synthesis of PBSFs. A two-step procedure, direct esterification followed by polycondensation, was employed to synthesize PBSF copolyesters, poly(butylene succinate) (PBS) and poly(butylene furandicarboxylate) (PBF) using a specially designed Inox 250 mL Autoclave-France reactor. The copolymers are named as PBSFφ_{FA}, where φ_{FA}% is the molar percentage of FA in feed, i.e., φ_{FA} mol % = FA/(SA + FA)·100%. The molar fraction of BF units, ϕ_{BF}, is defined as the copolymer composition.

For synthesis of PBSF10-50, FA (without purification), SA and BDO (diol/diacid molar ratio 1.5:1) were added into the reactor and then heated to 190 °C under stirring. The esterification reaction was conducted without catalyst at 190 °C for 2 h and then at 200 °C for another 2 h. Then, TBT (1.4 mmol/mol diacid) was added, and the esterification product was heated to 230 °C and polycondensed under vacuum at 230 °C for 1 h and then at 250 °C for another 4 h. PBS was also synthesized using the same procedure.

For PBSF60-90, FA (after purification), SA, BDO (diol/diacid molar ratio 2/1), and TBT were added into the reactor and then heated to 170 °C under stirring. The esterification reaction was conducted at 170 °C for 1 h, at 180 °C for 2 h and finally at 190 °C for 1 h. Extra BDO was added before the last hour, and the total diol/diacid ratio was 2.5/1. Then, $La(acac)_3$ (Ti/La 1/1 molar ratio) was added as a polycondensation catalyst, and the esterification product was heated to 230 °C and polycondensed under vacuum at 230 °C for 4 h and then at 250 °C for another 1 h. The same procedure was also used to synthesize PBF.

Characterization. The molecular weight distribution (MWD) of PBS and PBSF10-80 was measured at 30 °C with SEC (Agilent 1200 SEC) equipped with an Agilent-DRI refractive index detector and three columns: a PL gel 10 μm guard column and two PL gel Mixed-D 10 μm columns (linear columns of MWPS ranging from 500 to 10^6 g/mol). Chloroform was used as solvent. The concentration of sample solution was about 1 mg/mL, and the flow rate of the eluent was of 1 mL/min. Polystyrene standards were used for calibration. The MWD of PBSF90 and PBF was not measured with SEC because they are insoluble in chloroform.

The FTIR spectra were recorded with a Bruker Tensor 27 infrared spectrometer using a 5 mg/mL chloroform solution for PBS and PBSF10-80 and a 1,1,2,2-tetrachloroethane solution for BPSF90 and PBF. Different solvent were used here because of the different solubility of PBSFs depending on composition.

The ^{1}H NMR spectra were recorded with a NMR spectrometer (Bruker, 500 MHz), using deuterated chloroform ($CDCl_3$) or 1,1,2,2-tetrachloroethane ($C_2D_2Cl_4$) as solvent and tetramethylsilane (TMS) as an internal reference. The concentration of each sample solution was of about 17 mg/mL.

The thermal transitions were recorded with DSC on a Q200 thermal analyzer (TA Instruments) with a standard heating−cooling−heating mode. Both the heating and cooling rates were 10 °C/min. The starting and ending temperatures used depended on the composition, and details can be seen in the Results and Discussion section.

The thermal decomposition behavior was recorded with TGA (Q500, TA Instruments). The samples were heated from room temperature to 800 at 20 °C/min under N_2 atmosphere.

The tensile properties of PBSFs in full composition range except PBSF30 were measured with a Zwick Roell testing machine at 23 °C according to ASTM D638. Dumbbell-shaped specimens were prepared using a DSM Xplore Micro 3.5 cc injection molding machine and then conditioned at 23 °C and 50% relative humidity for over 48 h prior to testing. PBSF30 has very slow crystallization and low T_g, so it was very difficult to released from the mold after injection molding. Therefore, its tensile properties were not assessed. For each sample, at least five specimens were tested. The crosshead speed used was 50 mm/min for PBSF40−90 and 10 mm/min for other samples due to the great difference in the elongation at break. Additionally, for PBSFs with $\phi_{BF} \geq 60$ mol %, extra tensile testing was performed at a crosshead speed of 10 mm/min after the specimens were annealed at 60 °C for 2.5 h.

RESULTS AND DISCUSSION

Synthesis and Characterization. PBSF copolymers in full composition range were synthesized from SA, FA, and BDO by a two-step melt polycondensation procedure shown in Scheme 1.

Scheme 1. Synthesis of PBSF via Two-Step Melt Polycondensation of SA, FA, and BDO

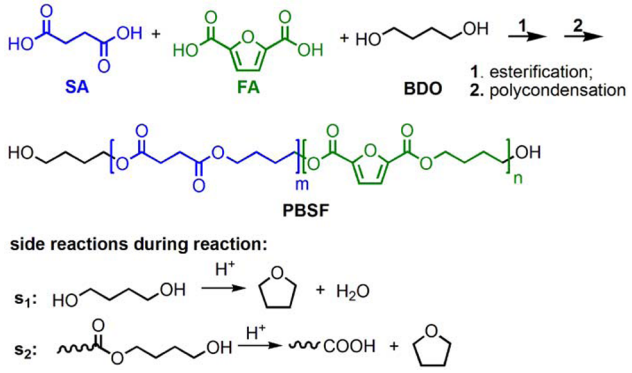

For PBS and PBSF10−50, the esterification reaction occurred readily with a diol/diacid molar ratio of 1.5/1 at 190−200 °C without catalyst. After esterification, TBT was added to catalyze the polycondensation reaction at higher temperature. Polymers with weight-average molecular weight (M_w) of 35000−65000 g/mol and polydispersity between 1.7 and 2.7 were obtained (see Table 1).

However, the syntheses of PBSF60−90 and PBF under the same conditions failed, and only polymers with M_w less than 10000 g/mol were obtained. The reason is attributed to incompletion of esterification reaction. In fact, in addition to the main esterification reaction, there were two tetrahydrofuran (THF)-forming side reactions during esterification stage (see Scheme 1). Through these reactions, BDO or even the esterification product (terminal hydroxybutyl ester) was converted into THF as a byproduct, which was distilled out of the reactor together with water. The side reactions were catalyzed by both acids. As FA has stronger acidity ($pK_a = 2.28$) than SA ($pK_{a1} = 4.2$, $pK_{a2} = 5.6$), they were accelerated with increasing φ_{FA}. This was supported by the experimental results shown in Figure 1. In synthesis of PBS, the amount of distillate reached the theoretical volume of byproduct water (18 mL, level 0) in 2 h, and then it increased very slowly to 19 mL within the next 2 h. It is supposed that about 2% BDO was converted into THF. Similar low THF formation was also

Table 1. Molecular Characteristics of PBS, PBSF Copolyesters and PBF

			NMR				SEC		
run	sample	φ_{FA}[c] (mol %)	ϕ_{BF}[d] (mol %)	$L_{n,BS}$[e]	$L_{n,BF}$[e]	R[f]	M_n (g/mol)	M_w (g/mol)	Đ[g]
0	PBS[a]	0	0				20500	35100	1.71
1	PBSF10[a]	10	9.72	6.24	1.13	1.05	22100	55800	2.52
2	PBSF20[a]	20	19.1	4.74	1.28	0.99	19900	51800	2.60
3	PBSF30[a]	30	30.5	2.92	1.44	1.04	22100	42900	1.94
4	PBSF40[a]	40	39.9	2.23	1.67	1.05	29000	65300	2.25
5	PBSF50[a]	50	49.5	1.86	1.92	1.06	18500	49000	2.65
6	PBSF60[b]	60	60.0	1.58	2.49	1.04	40800	89100	2.19
7	PBSF70[b]	70	70.9	1.37	3.31	1.03	22100	52400	2.38
8	PBSF80[b]	80	80.2	1.23	4.72	1.03	15700	38600	2.45
9	PBSF90[b]	90	89.7	1.11	7.83	1.03	nd[h]	nd[h]	nd[h]
10	PBF[b]	100	100				nd[h]	nd[h]	nd[h]

[a]Reaction conditions: (1) esterification: no catalyst, diol/diacid = 1.5, 190 °C/2 h + 200 °C/2 h; (2) polycondensation: TBT = 1.4 mmol/mol diacid, 230 °C/1 h + 250 °C/4 h. [b]Reaction conditions: (1) esterification: FA was purified before use, TBT = 1.4 mmol/mol diacid, diol/diacid = 2.5, 170 °C/1 h + 180 °C/2 h + 190 °C/1 h; (2) polycondensation: $La(acac)_3$, La/Ti = 1/1 molar ratio, 230 °C/4 h + 250 °C/1 h. [c]Molar percent of FA in feed. [d]Copolymer composition or molar percent of BF units in the copolymer. [e]Number-average length of BS and BF units, respectively. [f]Degree of randomness. [g]Polydispersity. [h]Not determined because of the insolubility of PBSF90 and PBF in chloroform.

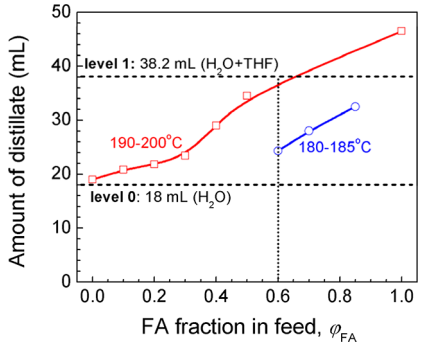

Figure 1. Dependence of the amount of distillate on FA molar fraction in feed (φ_{FA}) at the esterification stage (diol/diacid 1.5/1 mol/mol, 190−200 °C or 180−185 °C, 4 h). The dashed lines means theoretical amounts of distillate at different hypothetic cases: level 0: only water but no THF was formed; level 1: theoretical water plus THF formed from all excessive BDO.

reported in esterification of SA and BDO in previous literature.[26] However, in the presence of FA, the distillate amount increased with φ_{FA}, and with time during the whole esterification stage, suggesting that THF was formed continuously, especially at high φ_{FA}. Indeed, at φ_{FA} > 60%, the importance of collected distillate amount suggested that all excessive BDO (33%) was converted into THF (38.2 mL, level 1) at 190−200 °C. Thus, the esterification reaction was not completed, and the subsequent polycondensation reaction was slow or incomplete, and only low molecular weight products were obtained.

To succeed in synthesizing high-molecular-weight PBSF with φ_{FA} higher than 50%, the following measures were taken. First, TBT was added at the esterification stage, and the diol/diacid ratio was increased from 1.5 to 2.5 to accelerate the esterification reaction. Second, the esterification temperature was lowered down to depress the THF-forming side reactions. Third, $La(acac)_3$ was added at the second stage to catalyze polycondenation reaction together with TBT. The TBT-$La(acac)_3$ mixed catalyst was reported to be more reactive than the TBT single catalyst in synthesis of poly(butylene terephthalate),[27] and it was also used in synthesis of PBAT copolyester.[28] In addition, the polycondensation temperature/time program was changed, and FA was purified before use to further depress possible side reactions, which might result in thermal decomposition and coloration. The detailed conditions are described in the Experimental Section and also listed in Table 1. With these modifications, PBSF60−90 and PBF with M_w of 40 000−90 000 g/mol were successfully synthesized. All the polymers were produced in yield of 90−97%.

It was found that, depending on the composition, the solubility of PBSFs in common solvents changed. The copolyesters prepared with φ_{FA} no more than 80% can be dissolved in chloroform, but PBSF90 and PBF are insoluble. They can be dissolved in hot 1,1,2,2-tetrachloroethane at 50 °C. However, all the polymers remain insoluble in heptane and methanol.

In comparison to PBS, which is a white to slightly yellowish solid, the synthesized PBSFs and PBF are colored products. The coloration of PBSFs was also found to be composition dependent. The color darkens gradually with increasing φ_{FA}, and may be related to some impurities in the FA monomer. As a newly emerged biobased monomer, the purification problem of FA has not been completely solved yet. Therefore, dialkyl furandicarboxylates were used instead of FA itself in some R&D of other FA-based polyesters.[14,21,25] This is similar to the case during the early development of TPA-based polyesters in which dimethyl terephthalate was used instead of TPA. We selected the direct esterification and polycondensation route to synthesize PBSFs in this study because this route is usually characterized by simpler and easier separation of byproducts in industrial production. The catalyst, TBT, may also contribute to the coloration, as it is well-known that the use of TBT often results in yellowing of common polyesters.[29] When FA was purified with acetic acid before use and the polycondensation time at higher temperature (250 °C) was shortened from 4 to 1 h, the color of PBSFs (φ_{FA} ≥60 mol %) became paler to a certain extent as compared with the same PBSFs synthesized from FA without purification.

The chemical structure of the PBSFs was analyzed with FTIR and ^{1}H NMR. The FTIR spectra of PBS, PBSFs, and PBF are shown in Figure 2. The strong ester absorption ($\nu_{C=O}$) appears at 1714 cm^{-1} for PBS and shifts gradually to 1731 cm^{-1} for PBSFs. The absorption of terminal hydroxyl groups around 3430 cm^{-1} is very weak, indicating high molecular weights.

dx.doi.org/10.1021/bm301044f | Biomacromolecules 2012, 13, 2973−2981

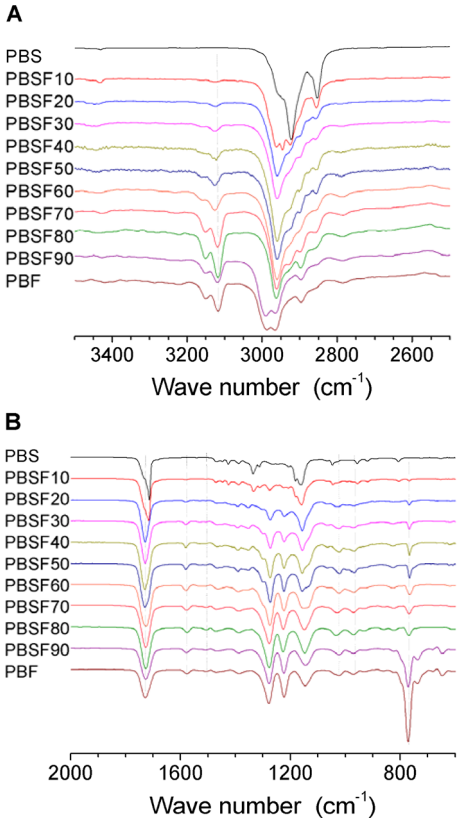

Figure 2. FTIR spectra of PBS, PBSF copolyesters, and PBF.

With comparison to PBS, some new absorption peaks appear for PBSFs, including ν_{C-H} of the furan ring at 3124 cm^{-1}, the furan C=C bond at 1582 cm^{-1} and 1508 cm^{-1}, furan breathing around 1022 cm^{-1}, and furan ring bending at 967 cm^{-1}, 826 cm^{-1} and 768 cm^{-1}.

The ^{1}H NMR spectra of PBS, PBSFs and PBF are shown in Figure 3, and the attributions of the chemical shifts are shown in Scheme 2 and Table 2. For PBS, the chemical shifts of CH_2 in SA unit (**s**) and CH_2 in BDO unit ($\mathbf{a}_1$ and $\mathbf{b}_1$) appear at 2.63 ppm, 4.11 ppm and 1.71 ppm, respectively. For PBSF, the chemical shifts of **s**, $\mathbf{a}_1$, and $\mathbf{b}_1$ are retained and some new chemical shifts appear: the C**H** in the furan ring at 7.21 ppm (**f**), the CH_2 in BDO unit close to different ester bonds resulting from copolycondensation at 4.15 ppm ($\mathbf{a}_2$), 4.36 ppm ($\mathbf{a}_3$) and 4.40 ppm ($\mathbf{a}_4$), and the middle CH_2 in BDO unit at 1.77($\mathbf{b}_2$), 1.85 ppm ($\mathbf{b}_3$) and 1.92 ppm ($\mathbf{b}_4$). It can also be seen that the peak areas of **s**, $\mathbf{a}_1$, and $\mathbf{b}_1$ decrease, and those of **f**, $\mathbf{a}_2$–$\mathbf{a}_4$, and $\mathbf{b}_2$–$\mathbf{a}_4$ increase with increasing φ_{FA}. For PBSF90 and PBF, deuterated 1,1,2,2-tetrachloroethane ($C_2D_2Cl_4$) was used as solvent because they are insoluble in $CDCl_3$. Accordingly,

Scheme 2. Chemical Structures of SBS, PBF, and SBF Units in PBSF Copolyesters

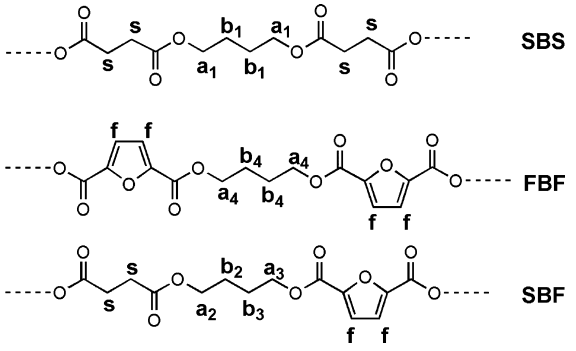

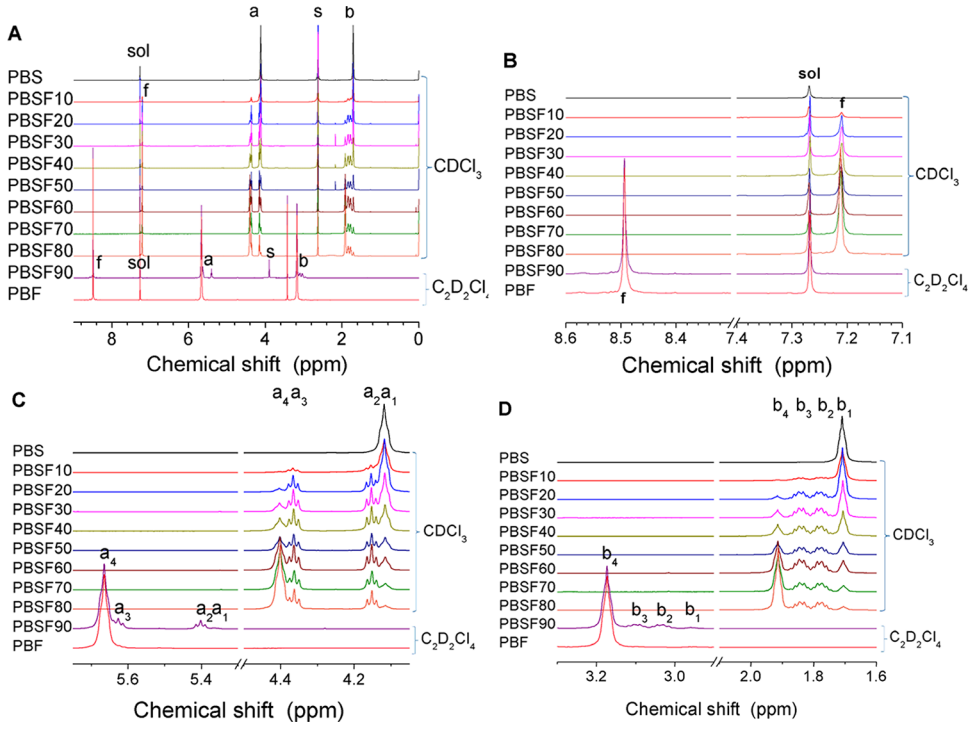

Figure 3. ^{1}H NMR spectra of PBS, PBSF copolyesters, and PBF. (A: the whole spectra; B–D: magnification of chemical shifts **f**, **a**, and **b**; solvent: $CDCl_3$ for PBS and PBSF10–80; $C_2D_2Cl_4$ for PBSF90 and PBF).

dx.doi.org/10.1021/bm301044f | Biomacromolecules 2012, 13, 2973–2981

Table 2. Attribution of Chemical Shifts (unit: ppm) of PBS, PBSF Copolyesters, and PBF

solvent	polymer	f	a_4	a_3	a_2	a_1	s	b_4	b_3	b_2	b_1
$CDCl_3$	PBS					4.11	2.63				1.71
	PBSF10−80	7.21	4.40	4.36	4.15	4.11	2.63	1.92	1.85	1.77	1.71
$C_2D_2Cl_4$	PBSF90	8.49	5.66	5.63	5.40	5.37	3.91	3.17	3.10	3.03	2.96
	PBF	8.49	5.66					3.17			

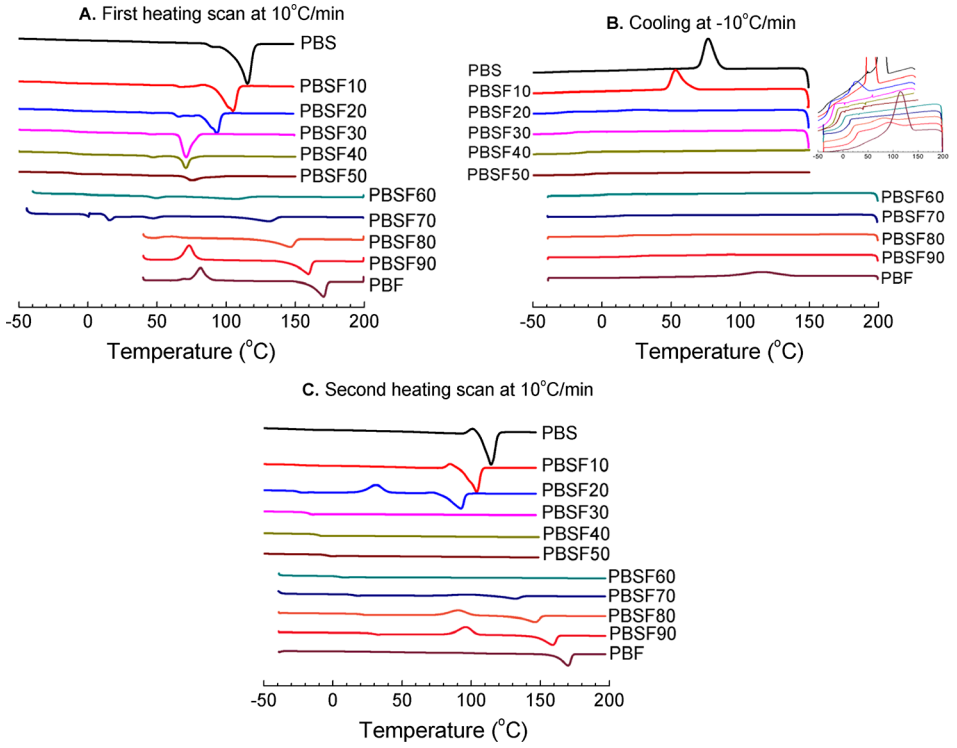

Figure 4. DSC curves of PBS, PBSF copolyesters, and PBF.

Table 3. Thermal Transition Properties of PBS, PBSF Copolyesters, and PBF

	first heating scan at 10 °C/min		cooling at 10 °C/min		second heating scan at 10 °C/min				
sample	T_m (°C)	ΔH_m (J/g)	T_c (°C)	ΔH_c (J/g)	T_g (°C)	T_{cc} (°C)	ΔH_{cc} (J/g)	T_m (°C)	ΔH_m (J/g)
PBS	115	112	76.6	75.9	−40.0			114	74.8
PBSF10	105	79.5	53.1	65.2	−25.0			104	61.9
PBSF20	93.1	60.8	25.2	9.6	−24.2	31.3	33.0	92.6	52.9
PBSF30	71.0	45.5			−17.3				
PBSF40	70.7	19.9			−10.5				
PBSF50	75.5	20.7			−3.5				
PBSF60	111	14.7			6.5				
PBSF70	131	28.9			14.6	97.8	10.7	132	13.7
PBSF80	147	34.3	76.3	2.6	22.0	91.2	26.8	146	27.5
PBSF90	159	37.9	88.2	5.0	30.5	96.2	30.2	159	36.1
PBF	170	45.8	115	41.6	44.8			170	42.2

the chemical shifts shift to low field. The details are listed in Table 2.

From the ^{1}H NMR spectra, the copolymer composition (ϕ_{BF}), the number-average sequence length of BS and BF units ($L_{n,BS}$ and $L_{n,BF}$), and the degree of randomness (R) are calculated using eqs 1−4, respectively, where the integrated intensity of chemical shift **i** is abbreviated as I_i.[30] The multipeaks fitting function of OriginPro 8.0 software was used to calculate the integrated intensity of the partially overlapped peaks a_1−a_4. The results are listed in Table 1. It can be seen that the ϕ_{BF} agrees well with the molar percentage of FA in diacid monomer feed, φ_{FA}. The $L_{n,BS}$ decreases and $L_{n,BF}$ increases with ϕ_{BF}, and they both approach to about 2 at ϕ_{BF} of 50 mol %. The copolyesters with $L_{n,BF}$ no more than 2 may be biodegradable,[31] and the biodegradability will be reported later. The degree of randomness is about 1, indicating random structure of the copolyesters. From the FTIR and ^{1}H NMR spectroscopic characterizations, it can be concluded that PBSF copolyesters with expected chemical structures have been successfully synthesized.

$$\phi_{BF}(\text{mol\%}) = 2I_f/(2I_f + I_s) \times 100\% \quad (1)$$

dx.doi.org/10.1021/bm301044f | Biomacromolecules 2012, 13, 2973−2981

$$L_{n,BS} = 1 + 2I_{a1}/(I_{a2} + I_{a3}) \quad (2)$$

$$L_{n,BF} = 1 + 2I_{a4}/(I_{a2} + I_{a3}) \quad (3)$$

$$R = 1/L_{n,BS} + 1/L_{n,BF} \quad (4)$$

Thermal Transition Behavior. The DSC scans of PBS, PBSFs, and PBF are shown in Figure 4, and the thermal transition data are summarized in Table 3. The composition dependences of melting temperature (T_m) and enthalpy (ΔH_m) and crystallization temperature (T_c) and enthalpy (ΔH_c) obtained from the second heating and cooling scans are shown in Figure 5A,B, respectively.

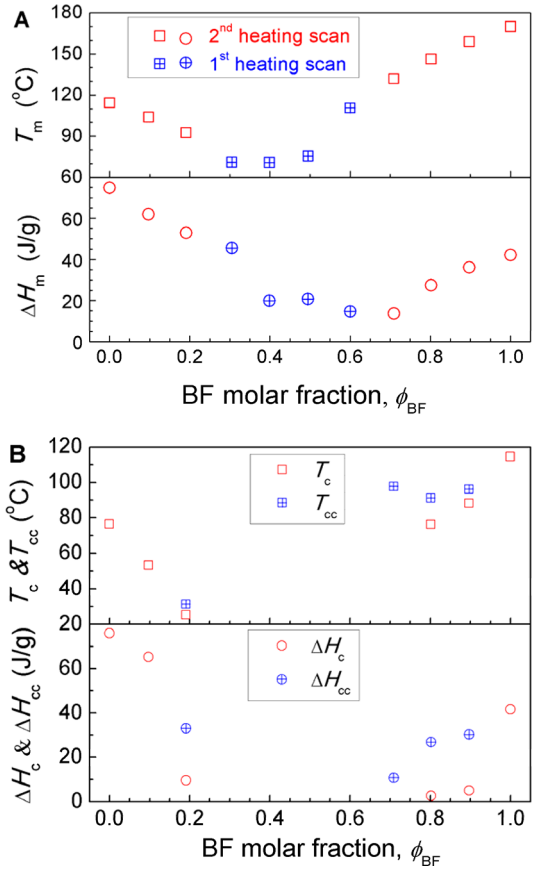

Figure 5. Composition dependences of (A) melting temperature (T_m) and melting enthalpy (ΔH_m) and (B) crystallization temperature (T_c and T_{cc}) and crystallization enthalpy (ΔH_c and ΔH_{cc}).

It can be seen that the thermal transition behavior of PBSF strongly depends on composition. The T_m, ΔH_m, T_c, and ΔH_c all decrease with ϕ_{BF} in the BS-rich composition range and increase upon further increasing ϕ_{BF}. PBS is a typical crystalline polymer. It exhibits high melt crystallization enthalpy (ΔH_c = 75.9 J/g) at 77 °C and high melting enthalpy (ΔH_m = 74.8 J/g) at 114 °C. Similar to PBS, PBSF10 also shows good melt crystallization ability (ΔH_c = 65.2 J/g, T_c = 53 °C) and high melting temperature (T_m = 104 °C). Melt crystallization of PBSF20 clearly weakened (ΔH_c = 9.6 J/g, T_c = 25 °C), but reasonably good cold crystallization (ΔH_{cc} = 33 J/g, T_{cc} = 31 °C) was observed in the second heating scan. The T_{cc} and ΔH_{cc} are also plotted in Figure 5B. For PBSFs30, 40, 50, and 60, neither melt crystallization in the cooling scan nor cold crystallization and melting in the second heating scan were observed because of very poor crystallization ability of the copolyesters. However, they can still crystallize slowly at the condition of natural cooling and therefore exhibit melting peaks at 71 °C (ΔH_m = 46 J/g), 71 °C (ΔH_m = 20 J/g), 75 °C (ΔH_m = 21 J/g), and 110 °C (ΔH_m = 15 J/g), respectively, in the first heating scans. For these polymers, the T_m and ΔH_m of the first scan are also plotted in Figure 5A to better understand their composition dependence. PBSF70 can not crystallize from melt but can cold crystallize at 10 °C/min. Like PBSF20, PBSF80 and PBSF90 have weak melt crystallizability but good cold crystallizability. Additionally, PBF shows high melt crystallization enthalpy (ΔH_c = 41.6 J/g, T_c = 115 °C) and high melting T_m (170 °C). In summary, the PBSF copolyesters can be classified into three types according to their melt crystallizability: PBS, PBSF10, and PBF (excellent to good), PBSF20 and PBSF70–90 (weak), and PBSF30–60 (very weak, nearly amorphous).

All the copolyesters have single glass transition temperature (T_g), in agreement with the random sequence structure validated by ^{1}H NMR. The T_g increases continuously with ϕ_{BF} (Figure 6). The well-known Fox equation (eq 5) can be

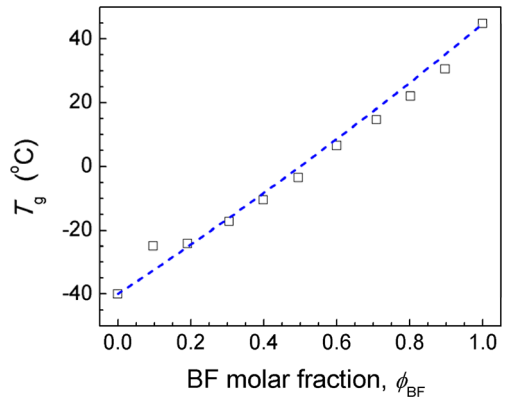

Figure 6. Composition dependence of the glass transition temperature (T_g) of PBSFs. The dashed line shows the values calculated using eq 5.

used to describe the composition dependence of T_g. The T_g of PBF (44.8 °C) is higher than the previously reported values (30.5 °C[19], 36 °C[20]), suggesting high molecular weight.

$$1/T_g = w_{BS}/T_{g,PBS} + w_{BF}/T_{g,PBF} \quad (5)$$

Thermal Stability. The TGA curves of PBS, PBSFs, and PBF are compared in Figure 7. The decomposition temperature at 5% weight loss, $T_{d,5\%}$ and decompostion temperature at the

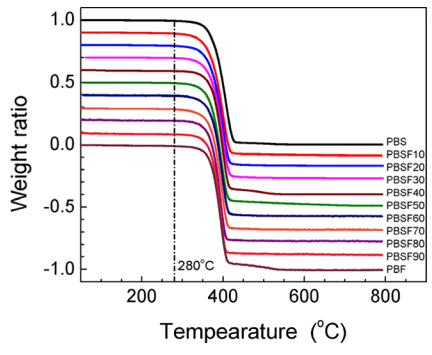

Figure 7. TGA thermograms of PBS, PBSF copolyesters, and PBF (N_2, heating rate 20 °C/min).

dx.doi.org/10.1021/bm301044f | Biomacromolecules 2012, 13, 2973–2981

maximum rate, $T_{d,max}$ are listed in Table 4. The $T_{d,5\%}$ and $T_{d,max}$ of PBS, PBST, and PBAT (Ecoflex) reported in the literature[32]

Table 4. Characteristic Decomposition Temperatures $T_{d,5\%}$ and $T_{d,max}$ of PBS, PBSFs, and PBF Determined by TGA[a]

polymer	$T_{d,5\%}$ (°C)	$T_{d,max}$ (°C)	polymer	$T_{d,5\%}$ (°C)	$T_{d,max}$ (°C)
PBS	352	407	PBSF60	345	398
PBS[b]	363	399	PBSF70	339	397
PBSF10	339	400	PBSF80	347	394
PBSF20	342	399	PBSF90	345	395
PBSF30	344	400	PBF	350	395
PBSF40	349	399	PBST50–70[b]	374–380	396–408
PBSF50	344	396	Ecoflex[b]	375	402

[a]N_2, 20 °C/min. [b]Data cited from ref 32.

are also compared in the table. Weight loss does not take place for all synthesized polymers before 280 °C under N_2 atmosphere. The PBSFs and PBF have nearly composition-independent $T_{d,5\%}$ and $T_{d,max}$. The averages of $T_{d,5\%}$ and $T_{d,max}$ are 344 ± 4 °C and 397 ± 2 °C, respectively. In comparison, the $T_{d,5\%}$ and $T_{d,max}$ of PBS, PBST, and Ecoflex are 352 °C and 407 °C, 374–380 °C and 396–408 °C, and 375 °C and 402 °C, respectively.[32] These results indicate that PBSFs have excellent thermal stability, although it is slightly lower than the stability of PBS, PBST, and Ecoflex. Also, the residue $La(acac)_3$ catalyst does not show an observable effect on the thermal stability.

Mechanical Properties. The tensile properties, namely, modulus (E), strength at break (σ_b), and elongation at break (ε_b), are shown in Figure 8. The tensile properties of PBS (E = 680 MPa, σ_b = 30 MPa and ε_b = 130%) are comparable to those of commercial PBS.[33,34] In comparison with PBS, PBF has much higher modulus (1.8 GPa), better strength (35 MPa), but much lower elongation at break (2.5%). The modulus and strength are much higher than the previously reported values for PBF (1.1 GPa and 20 MPa[17]), possibly because of higher molecular weight, and the elongation is comparable to the previously reported value (2.8%[17]). At ϕ_{BF} from 0 mol % to 40 mol %, the modulus and strength of PBSFs decrease, and the elongation increases because the crystallizability decreases with ϕ_{BF} as discussed above. PBSF10 and PBSF20 exhibit good tensile modulus (360–550 MPa) and strength (~20 MPa) and moderate elongation at break (160–320%). PBSF40–50 are nearly amorphous polymers with low T_g (−10 to −3.5 °C) and therefore have much lower tensile modulus and high elongation (580–660%). At ϕ_{BF} from 50 mol % to 100 mol %, the overall trend is that the tensile modulus and strength increase and elongation at break decreases, but the composition dependence appears to be complicated: PBSF60 has unexpectedly high tensile strength and PBSF80 has much lower modulus and strength than expected. The high tensile strength of PBSF60 may result from its highest molecular weight (see Table 1). PBSF80 has low modulus and strength, possibly because of poor melt crystallization after injection molding.

To better interpret the composition dependence of the mechanical properties of PBSFs, the thermal transition of the specimens used for tensile testing was measured by DSC. The DSC curves are shown in Figure 9. The net melting enthalpy $\Delta H_{m,net}$, namely, the melting enthalpy minus crystallization enthalpy ($\Delta H_{m,net} = \Delta H_m - \Delta H_c$, if cold crystallization occurred), is also plotted and used to roughly present the crystallinity of the specimens. PBSF80, PBSF90 and PBF exhibited clear cold crystallization in the heating scan and low $\Delta H_{m,net}$, indicating they did not crystallize completely from melt after injection molding. PBSF80 has poor crystallization

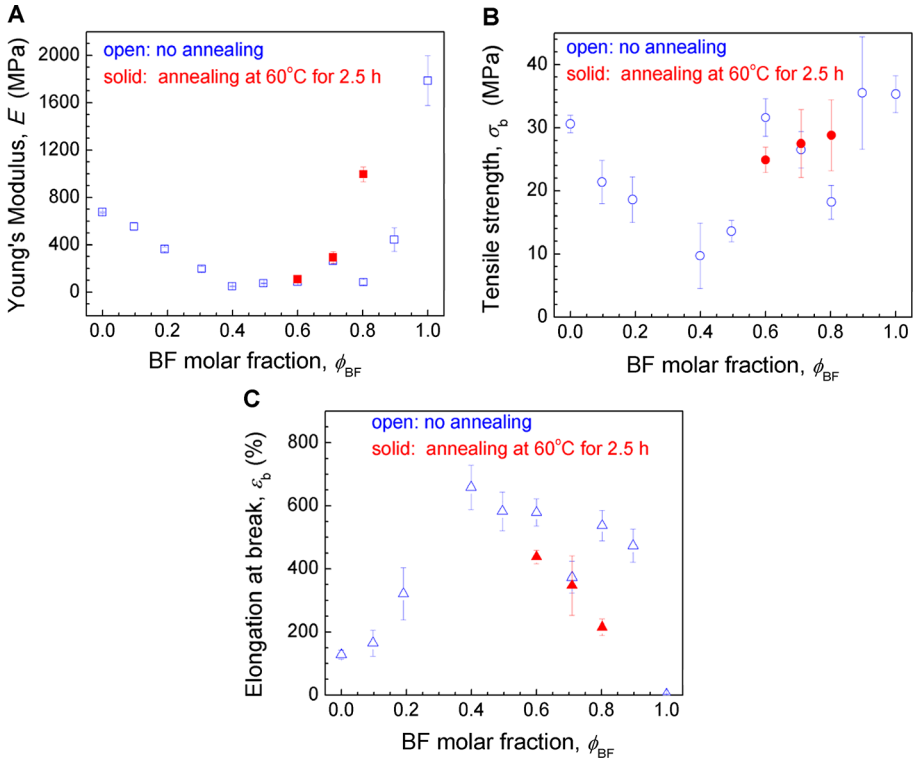

Figure 8. Composition dependence of (A) modulus, (B) strength, and (C) elongation at break of PBSF in tensile testing.

dx.doi.org/10.1021/bm301044f | Biomacromolecules 2012, 13, 2973–2981

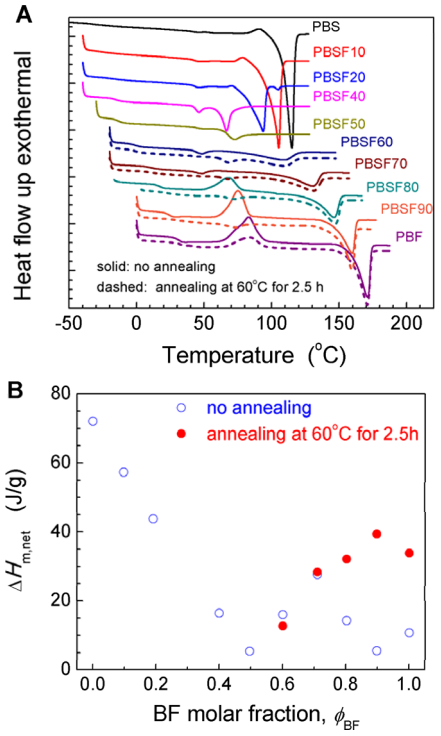

Figure 9. (A) DSC curves of the specimens used for tensile testing without or with annealing at 60 °C for 2.5 h, and (B) the net melting enthalpy ($\Delta H_{m,net} = \Delta H_m - \Delta H_c$) of the specimens.

and low T_g (22 °C) close to the testing temperature (23 °C) so that it has low tensile strength and large elongation at break. PBSF90 and PBF have T_g higher than the testing temperature, and therefore, have higher modulus and strength than PBSF80.

To further understand the effect of crystallization on mechanical properties, extra tensile testing of the specimens with ϕ_{BF} of 60−100 mol % were performed after annealed at 60 °C for 2.5 h. The tensile properties and DSC results are also plotted in Figures 8 and 9, respectively. For PBSF60, its $\Delta H_{m,net}$ decreased a little after annealing, and its tensile strength decreased accordingly. The $\Delta H_{m,net}$ of PBSF70 remained unchanged after annealing, so the mechanical properties remained unchanged too. However, the $\Delta H_{m,net}$ of PBSF80 increased clearly after annealing, therefore its modulus and strength increase, and its elongation at break decreases significantly. The $\Delta H_{m,net}$ of PBSF90 and PBF also increased clearly, but they became too brittle to perform tensile testing, as they were broken when fixed in the grips.

In summary, the mechanical properties of PBSF copolyesters depend on their molecular weight, composition, T_g, as well as crystallinity or thermal history, especially for the slowly crystallized copolyesters. The copolyesters exhibit tensile properties ranging from crystalline thermoplastics ($\phi_{BF} \leq$ 20% and ∼100%) to nearly amorphous elastomer-like polymers (ϕ_{BF} 40−60%). Indeed, PBSFs40−60 do exhibit some rebound resilience. Therefore, as counterparts of PBST, these new copolyesters may find end applications from thermoplastics to elastomers or impact modifiers for other polymers.

CONCLUSIONS

Novel aliphatic-aromatic random copolyesters, PBSFs in full composition range were successfully synthesized from FA, SA, and BDO via a direct esterification and polycondensation process using TBT or TBT/La(acac)$_3$ as catalyst. The copolyesters have the expected chemical structure and their copolymer composition is determined by the feed ratio of the two diacid monomers. They have excellent thermal stability. The T_g increases continuously with BF unit content (ϕ_{BF}). Both crystallizability and T_m of PBSF decrease with ϕ_{BF} in the BS-rich composition range, but rise again in the BF-rich range. The very BS-rich or BF-rich copolyesters are crystalline polymers, but the copolyesters with intermediate composition (ϕ_{BF} 40−60%) are close to amorphous polymers. The mechanical properties depend on molecular weight, T_g, composition, crystallinity, and thermal history. On the whole, the tensile modulus and strength decrease with ϕ_{BF} in the 0−40% range, but rise again in the 50−100% range. The variation trend of elongation at break goes just the opposite.

As new potentially biobased copolyesters, PBSFs have tunable properties ranging from crystalline polymers possessing good tensile modulus (360−1800 MPa) and strength (20−35 MPa) to nearly amorphous polymers possessing low T_g and very high elongation (∼600%). Therefore, they may find applications as thermoplastics as well as elastomers or impact modifiers. Additionally, they may be biodegradable in the appropriate composition range. Further research is under way and will be reported later.

AUTHOR INFORMATION

Corresponding Author

*Tel: +32(0)65 37 34 80; Fax: +32(0)65 37 34 84; E-mail: philippe.dubois@umons.ac.be.

Notes

The authors declare no competing financial interest.

ACKNOWLEDGMENTS

This work was supported by the European Commission and Région Wallonne FEDER program (Materia Nova) and OPTI^{2}MAT program of excellence, and by the Interuniversity Attraction Pole program of the Belgian Federal Science Policy Office (PAI 6/27). L.W. also thanks the Belgium FNRS-FRFC, the National Basic Research Program of China (973 Program, 2011CB606004), the National Key Technology R&D Program of China (2012BAD11B03), the National Nature Science Foundation of China (21074109), and the Fundamental Research Funds for the Central Universities of China for supporting his visiting research at UMONS.

REFERENCES

(1) Coombs, J.; Hal, K. *Renew. Energ.* **1998**, *15*, 54−59.
(2) Bozell1, J. J. *Clean* **2008**, *36*, 641−647.
(3) Nikolau, B. J; Perera, M. A. D. N.; Brachova1, L.; Shanks, B. *Plant J.* **2008**, *54*, 536−545.
(4) Williams, C. K.; Hillmyer, M. A. *Polym. Rev.* **2008**, *48*, 1−10.
(5) van Beilen, J. B.; Poirier, Y. *Plant J.* **2008**, *54*, 684−701.
(6) Belgacem, M. N., Gandini, A., Eds. *Monomers Polymers and Composites from Renewable Resources*; Elsevier: Amsterdam, 2008.
(7) Albertsson, A.-C.; Varma, I. K. *Adv. Polym. Sci.* **2002**, *157*, 1−40.
(8) Drumright, R. E.; Gruber, P. R.; Henton, D. E. *Adv. Mater.* **2000**, *12*, 1841−1846.
(9) Top Value Added Chemicals from Biomass Volume I−Results of Screening for Potential Candidates from Sugars and Synthesis Gas, http://www1.eere.energy.gov/biomass/pdfs/35523.pdf. Accessed April 5, 2005.
(10) Kröger, M.; Prüße, U.; Vorlop, K.-D. *Top. Catal.* **2000**, *13*, 237−242.

(11) Koopman, F.; Wierckx, N.; de Winde, J. H.; Ruijssenaars, H. J. *Bioresour. Technol.* **2010**, *101*, 6291−6296.
(12) Boisena, A.; Christensena, T. B.; Fub, W.; Gorbanevc, Y. Y.; Hansenc, T. S.; Jensenb, J. S.; Klitgaardc, S. K.; Pedersena, S.; Riisagerc, A.; Ståhlbergc, T.; Woodleyb, J. M. *Chem. Eng. Res. Des.* **2009**, *87*, 1318−1327.
(13) Moreaua, C.; Belgacemb, M. N.; Gandini, A. *Top. Catal.* **2004**, *27*, 11−30.
(14) de Jong, E. Furanics: Versatile Molecules Applicable for Biopolymers Applications. http://www.fib2010.org/Resources/fib-de%20Jong,%20Ed.pdf. Accessed July 5, 2011.
(15) Oore, J. A. *Macromolecules* **1978**, *11*, 568−573.
(16) Storbeck, R.; Ballauff, M. *Polymer* **1993**, *34*, 5003−5006.
(17) Gandini, A.; Silvestre, A. J. D.; Neto, C. P.; Sousa, A. F.; Gomes, M. *J. Polym. Sci., Part A: Polym. Chem.* **2009**, *47*, 295−298.
(18) Gomes, M.; Gandini, A.; Silvestre, A. J. D.; Reis, B. *J. Polym. Sci., Part A: Polym. Chem.* **2011**, *49*, 3759−3768.
(19) Jiang, M.; Liu, Q.; Zhang, Q.; Ye, C.; Zhou, G. Y. *J. Polym. Sci., Part A: Polym. Chem.* **2012**, *50*, 1026−1036.
(20) Ma, J. P.; Pang, Y.; Wang, M.; Xu, J.; Ma, H.; Nie, X. *J. Mater. Chem.* **2012**, *22*, 3457−3461.
(21) Grosshardt, O.; Fehrenbacher, U.; Kowollik, K.; Tübke, B.; Dingenouts, Nico.; Wilhelm, M. *Chem. Ing. Tech.* **2009**, *81*, 1829−1835.
(22) Ki, H. C.; Park, O. O. *Polymer* **2001**, *42*, 1849−1861.
(23) Witt, U; Yamamoto, M.; Seeliger, U.; Müller, R. J.; Warzelhan, V. *Angew. Chem., Int. Ed.* **1999**, *38*, 1438−1442.
(24) Nagataa, M.; Gotob, H.; Sakaib, W.; Tsutsumib, N. *Polymer* **2000**, *41*, 4373−4376.
(25) Oishi, A.; Iida, H.; Taguchi, Y. *Kobunshi Ronbunshu* **2010**, *67*, 541−543.
(26) Hu, L. X.; Wu, L. B.; Song, F. C.; Li, B.-G. *Macromol. React. Eng.* **2010**, *4*, 621−632.
(27) Banach, T. E.; Berti, C.; Colonna, M.; Fiorini, M.; Marianucci, E.; Messori, M.; Pilati, F.; Toselli, M. *Polymer* **2001**, *42*, 7511−7516.
(28) Han, L.; Zhu, G. X.; Wang, W.; Chen, W. *J. Appl. Polym. Sci.* **2009**, *113*, 1298−1306.
(29) Scheirs, J., Long, T. E., Eds. *Modern Polyesters: Chemistry and Technology of Polyesters and Copolyesters*; John Wiley & Sons: West Sussex, U.K., 2003.
(30) Chen, X. R.; Chen, W.; Zhu, G. X.; Huang, F. X.; Zhang, J. C. *J. Appl. Polym. Sci.* **2007**, *104*, 2643−2649.
(31) Witt, U.; Miiller, R.-J.; Deckwer, W.-D. *Macrornol. Chem. Phys.* **1996**, *197*, 1525−1535.
(32) Luo, S. L.; Li, F. X.; Yu, J. Y. *J. Polym. Res.* **2011**, *18*, 393−400.
(33) Xu, J.; Guo, B.-H. *Biotechnol. J.* **2010**, *5*, 1149−1163.
(34) Biosafe extrusion grade, http://www.xinfupharm.com/ProductView-xf.asp?ID=164. Accessed August 22, 2008.